

OPEN ACCESS

Effective-range description of a Bose gas under strong one- or two-dimensional confinement

To cite this article: Pascal Naidon *et al* 2007 *New J. Phys.* **9** 19

View the [article online](#) for updates and enhancements.

You may also like

- [Detection of C₂O in IRC +10216: Oxygen-Carbon Chain Chemistry in the Outer Envelope](#)
E. D. Tenenbaum, A. J. Apponi, L. M. Ziurys *et al.*
- [Structure and Dynamics of Self-Assembled Mercaptobenzimidazole Monolayers on Au\(111\)](#)
Liang Yueh Ou Yang and Thomas P. Moffat
- [Enhanced Black Hole Mergers in Active Galactic Nucleus Disks due to Precession-induced Resonances](#)
Hareesh Gautham Bhaskar, Gongjie Li and Douglas Lin

Effective-range description of a Bose gas under strong one- or two-dimensional confinement

Pascal Naidon¹, Eite Tiesinga¹, William F Mitchell²
and Paul S Julienne¹

¹ Atomic Physics Division, National Institute of Standards and Technology,
100 Bureau Drive Stop 8423, Gaithersburg, MD 20899-8423, USA

² Mathematical and Computational Sciences Division, National Institute of
Standards and Technology, 100 Bureau Drive Stop 8910, Gaithersburg,
MD 20899-8910, USA

E-mail: pascal.naidon@nist.gov

New Journal of Physics **9** (2007) 19

Received 14 July 2006

Published 29 January 2007

Online at <http://www.njp.org/>

doi:10.1088/1367-2630/9/1/019

Abstract. We point out that theories describing *s*-wave collisions of bosonic atoms confined in one-dimensional (1D) or two-dimensional (2D) geometries can be extended to much tighter confinements than previously thought. This is achieved by replacing the scattering length by an energy-dependent scattering length which was already introduced for the calculation of energy levels under 3D confinement. This replacement accurately predicts the position of confinement-induced resonances in strongly confined geometries.

Many experiments investigating the properties of cold atomic gases and Bose–Einstein condensates are now performed in tightly confining traps, such as tight optical lattices, leading to systems of reduced dimensionality [1]–[4]. There are many uses for such confinements. In spectroscopic measurements, they eliminate unwanted Doppler and recoil effects [5, 6]. They can also be used to create tunable analogues of condensed matter systems, and give the possibility to investigate remarkable many-body regimes in low dimensions such as the Tonks–Girardeau gas [7]–[10]. The theory of *s*-wave atomic collisions in strongly confined systems has been established in [7, 11] for one-dimensional (1D) and two-dimensional (2D) confinement, respectively. Both predict a confinement-induced resonance of the effective 1D or 2D interaction strength. These predictions rely on a description of the atomic interaction in terms of the scattering length only. However, in 3D confined systems, it was shown that a more refined description is needed for very tight confinement [12, 13]. Similarly, in 2D confined systems, numerical calculations in [14] showed that the scattering length description of [7] may be insufficient.

In this paper, we present an accurate analytical description for scattering in 1D and 2D geometries based on the findings of [13, 14].

We consider a gas of bosonic atoms in an optical lattice and assume that there is little tunnelling between the lattice cells, so that each cell is independent. The atoms in a cell are confined by a trapping potential which will be assumed harmonic (which is true near the centre of the cell). Let us consider a pair of atoms in such a cell. For a harmonic potential, the centre-of-mass motion decouples from the relative motion and the stationary Schrödinger equation for the relative motion wave function $\psi(\vec{r})$ reads

$$\left[-\frac{\hbar^2}{2\mu} \nabla_{\vec{r}}^2 + U(r) + V(\vec{r}) \right] \psi(\vec{r}) = E\psi(\vec{r}). \quad (1)$$

Here, $\vec{r} = (x, y, z)$ is the relative coordinate with separation r , μ the reduced mass, $U(r)$ the isotropic atom–atom interaction potential, $V(\vec{r})$ the trapping potential, and E the relative energy.

For 2D confinement (*tube* or *wave guide* geometry), the atoms are strongly confined in the xy -directions and (almost) free to move in the z -direction, therefore we set

$$V(\vec{r}) \equiv V_{2D}(\vec{r}) = \frac{1}{2}\mu\omega^2\rho^2,$$

where $\rho = \|\vec{\rho}\|$ and $\vec{\rho}$ is the projection of \vec{r} on the xy -plane. For 1D confinement (*pancake* geometry), the atoms are strongly confined in the z -direction and (almost) free to move in the xy -directions

$$V(\vec{r}) \equiv V_{1D}(\vec{r}) = \frac{1}{2}\mu\omega^2z^2.$$

Here, ω is the trapping frequency at the centre of the cell and we define $\sigma = \sqrt{\hbar/(2\mu\omega)}$ as the typical length scale associated to the trap in the confined directions.

Any scattering solution $\psi(\vec{r})$ of equation (1) is composed of an incident wave and a scattered wave. A plane wave basis can be used for the incident wave, and the scattered wave can be expressed with the noninteracting Green's function $G(\vec{r}, \vec{r}')$ of the system for $U(r) = 0$. Namely, for 2D confinement, one has

$$\psi(\vec{r}) = \phi_{nm}(\vec{\rho}) e^{iq_{nm}z} - \int G_{2D}(\vec{r}, \vec{r}') U(r') \psi(\vec{r}') d^3\vec{r}', \quad (2)$$

where $\phi_{nm}(\vec{\rho})$ denotes the unit-normalized 2D isotropic harmonic oscillator eigenstate of principal quantum number n and angular quantum number m , and $q_{nm} = \sqrt{(2\mu/\hbar^2)E - (2n + 1 + |m|)/\sigma^2}$ is the wavenumber of the incident plane wave. The Green's function reads

$$G_{2D}(\vec{r}, \vec{r}') = \sum_{v,\mu} \phi_{v\mu}(\vec{\rho}) \phi_{v\mu}(\vec{\rho}') \frac{e^{iq_{v\mu}|z-z'|}}{2iq_{v\mu}}.$$

For 1D confinement, one has

$$\psi(\vec{r}) = \varphi_n(z) e^{i\vec{q}_n \cdot \vec{\rho}} - \int G_{1D}(\vec{r}, \vec{r}') U(r') \psi(\vec{r}') d^3\vec{r}', \quad (3)$$

where $\varphi_n(z)$ denotes the unit-normalized 1D harmonic oscillator eigenstate of vibrational index n , and \vec{q}_n is the wavevector of the incident plane wave with norm $q_n = \sqrt{(2\mu/\hbar^2)E - (n + (1/2))/\sigma^2}$. The Green's function reads

$$G_{\text{1D}}(\vec{r}, \vec{r}') = \sum_{\nu} \varphi_{\nu}(z)\varphi_{\nu}(z') \frac{i}{4} H_0^{(1)}(q_{\nu}|\rho - \rho'|)$$

where $H_{\alpha}^{(1)}$ is the first Hankel function.

We first assume that the interaction potential $U(r)$ has a finite range r_b . This means that there is a separation $r_0 \gg r_b$ beyond which the wavefunction is essentially a solution of equation (1) with $U(r) = 0$, that is to say a solution of the noninteracting problem. This is indeed the case for typical atomic interactions which drop off as $-C_6/r^6$ van der Waals potentials. Because of this fast drop-off, the wavefunction (at sufficiently low energy) reaches its noninteracting form for $r^4 \gg (1/20)\beta_6^4$, where $\beta_6 = (2\mu C_6/\hbar^2)^{1/4}$ [16]. The separation r_0 is therefore on the order of β_6 , which ranges typically from 2 to 5 nm.

We further assume that the interaction potential U scatters only s -waves. The scattering of partial waves of arbitrary order under cylindrical confinement was treated in detail in [17]. Retaining only s -wave scattering is valid in the absence of shape resonances and if the cold-collision condition $kr_0 < 1$ is satisfied, where $\hbar k = \sqrt{2\mu E}/\hbar$ is the collisional momentum (see appendix).

Under these two assumptions, the noninteracting form of equations (2) and (3) is obtained by first taking the limit $r \gg r'$ of the Green's function (since $r > r_0 \gg r_b \sim r'$) and then approximating the remaining integral over \vec{r}' by $\phi_{\nu,\mu}(0)$ (or $\varphi_{\nu}(0)$) times a quantity $4\pi A$ which does not depend on the indices ν or μ appearing inside the Green's function (taking into account the dependence on ν, μ would introduce higher-order partial wave scattering [17] — see appendix). These two steps are formally equivalent to taking the Green's function out of the integral in equations (2) and (3) and evaluate it at $r' = 0$. Note that this can be achieved at any r by replacing the potential $U(r)$ by a regularized contact interaction [18]. For 2D confinement, one finds [19]

$$\psi(\vec{r}) \underset{r>r_0}{=} \phi_{nm}(\vec{\rho}) e^{iq_{nm}z} - 4\pi A_{nm} \sum_{\nu,\mu} \phi_{\nu\mu}(\vec{\rho}) \phi_{\nu\mu}(0) \frac{e^{iq_{\nu\mu}|z|}}{2iq_{\nu\mu}} \quad (4)$$

and for 1D confinement [7],

$$\psi(\vec{r}) \underset{r>r_0}{=} \varphi_n(z) e^{i\vec{q}_n \times \vec{\rho}} - 4\pi A_n \sum_{\nu} \varphi_{\nu}(z) \varphi_{\nu}(0) \frac{i}{4} H_0^{(1)}(q_{\nu}\rho), \quad (5)$$

where the factors A_{mn} and A_n are to be determined.

The wavefunction ψ can also be expanded in spherical partial waves

$$\psi(\vec{r}) = \sum_{\ell=0}^{\infty} \sum_{m=-\ell}^{\ell} \psi_{\ell,m}(r) Y_{\ell,m}(\theta, \varphi), \quad (6)$$

where $Y_{\ell,m}$ are the spherical harmonics and θ the angle between \vec{r} and the z -axis, φ the angle between $\vec{\rho}$ and the x -axis. At short separations, the confining potential $V(\vec{r})$ is negligible, so one can expect that within a certain range r_1 related to the confinement length σ (see appendix),

the wavefunction is close to a solution of equation (1) with $V(\vec{r}) = 0$, that is to say, a solution of the free-space scattering problem. Beyond r_0 , the partial waves of this solution reach their noninteracting form which is known to be a combination of regular and irregular spherical Bessel functions. Consistent with the s -wave approximation, there is no irregular Bessel function for $\ell \neq 0$, i.e. no scattered partial wave. For the s -wave ($\ell = 0$), we have

$$\psi_{00}(r) = \eta \left(\frac{\sin kr}{kr} - a(k) \frac{\cos kr}{r} \right) \quad \text{for } r_0 < r < r_1, \quad (7)$$

where η is a normalization factor to be determined and $a(k) = -\tan \delta_k/k$ is the energy-dependent s -wave scattering length introduced in [13, 15] (δ_k is the usual s -wave phase shift, related to the s -wave component of the reactance matrix $K_s(k) = -\tan \delta_k$). This energy-dependent scattering length contains all the effects of the interaction on the wavefunction in the region $r_0 < r < r_1$, and for any collisional energy E . For moderately tight traps $\sigma \gg r_0$ leading to small collisional energies, there is a range of r for which equation (7) simplifies to

$$\psi(\mathbf{r}) = \eta \left(1 - \frac{a}{r} \right), \quad (8)$$

where $a = \lim_{k \rightarrow 0} a(k)$ is the scattering length of the potential. However, for very tight lattices, σ may be close to r_0 and only equation (7) holds.

The essence of the method used in [7, 19] is to assume that $\sigma \gg r_0$ and match the noninteracting expressions (4) and (5), respectively, with the free-space expression (8) in the region $r_0 < r < r_1$ where they both are valid. (In [7], this is implicitly achieved by use of a 3D regularized contact interaction.) By performing the matching procedure up to zeroth order in the asymptotic expansion in r/σ near $r = 0$, they obtain two relations yielding the two unknown factors η and A_{nm} (or A_n). From that knowledge, they deduce the effective 1D and 2D interaction strengths in the quasi-1D or 2D regime ($q_n, q_{nm} \ll k$)

$$g_{1D} = \frac{\hbar^2}{\mu\sigma} \left(\frac{\sigma}{a} + \frac{\zeta(1/2)}{\sqrt{2}} \right)^{-1}, \quad (9)$$

$$g_{2D} = 4\pi \frac{\hbar^2}{\mu} \left(\frac{\sqrt{2\pi}\sigma}{a} + \ln \left(\frac{B}{\pi q_0^2 \sigma^2} \right) \right)^{-1}, \quad (10)$$

with $B \approx 0.915$ and $\zeta(1/2)/\sqrt{2} \approx -1.033$, where ζ is the Riemann zeta function. The singularity in these expressions as a function a , σ , or q_0 corresponds to the confinement-induced resonance. Note, however, that these analytical formulae are valid only when σ is large with respect to r_0 .

We stress here that the method can be extended by matching the s -wave component of the noninteracting expressions (4) or (5) with the more general free-space expression (7). It is straightforward to see that a matching to zeroth order in r/σ results in the same conditions as those of [7, 19], but with the scattering length a being replaced by the energy-dependent $a(k)$ in all the formulae. In particular, a is replaced by $a(k)$ in the expressions for η , A_{nm} , A_n and equations (9) and (10). Surprisingly, we find that once the two unknown factors η and A_{nm} (or A_n) are determined this way, the expression (4) or (5) match the expression (7) up to second order in r/σ , i.e. the next two orders automatically match without the need for extra parameters. This was checked numerically both in 2D and 1D confinement, and we give in the appendix

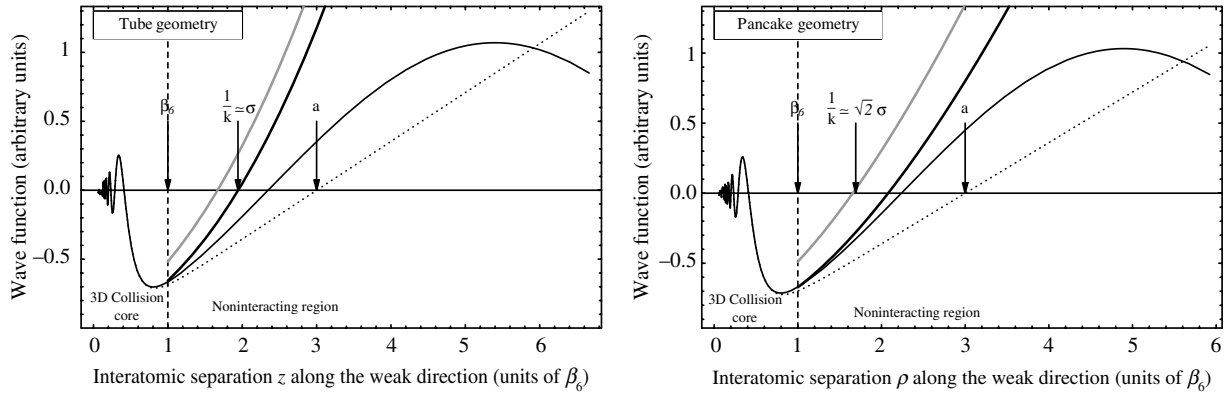


Figure 1. Cut through the function $r\psi(\vec{r})$ in a confined geometry for a van der Waals interaction with scattering length $a = 3\beta_6$, where $\beta_6 = (2\mu C_6/\hbar^2)^{1/4}$ is the van der Waals length. We have chosen $a = 3\beta_6$ as an illustrative value; for comparison, $a \approx 0.6\beta_6$ for ^{87}Rb , $a \approx -10\beta_6$ for ^{133}Cs , and $a > 4\beta_6$ for ^{86}Sr . Left panel: function $z\psi(\rho = 0, z)$ as a function of z for 2D confinement (tube) with $\sigma = 1.95\beta_6$. Right panel: function $\rho\psi(\rho, z = 0)$ as a function of ρ for 1D confinement (pancake) with $\sigma = 1.18\beta_6$. In both panels, the s -wave component of the solution to the free-space scattering problem at energy $E = \hbar^2 k^2/2\mu$ is represented as a thin black line. For $r > \beta_6$ it has the asymptotic form corresponding to equation (7). The thick black line represents the 1D or 2D wavefunction in the noninteracting region obtained from equation (4) or (5). It is determined by a matching procedure with the free-space scattering wavefunction, as explained in the text. The previous theories [7, 11] were based on a matching with the solution to free-space scattering at zero energy (dotted line), which has the asymptotic form corresponding to equation (8) for $r > \beta_6$. The resulting noninteracting 1D and 2D wave functions are represented by thick grey lines. They do not connect to the zero-energy wave function for the considered confinements. The lengths β_6 , a and $1/k$ are indicated by arrows.

an analytical derivation of this result for 2D confinement, based on mathematical assumptions which we checked numerically. As a result, the expressions (4) or (5) and (7) can be matched within less than 1% for $\sigma \gtrsim r_0$. In figure 1, we illustrate the matching of the wavefunctions for a confinement σ close to r_0 , in the case of a van der Waals interaction $U(r) = -\frac{C_6}{r^6}$, for which $r_0 \approx \beta_6$, as stated earlier. The figure shows both the s -wave component of the solution to the 3D free-space problem (which is highly oscillatory for $r < r_0$, and has the asymptotic form (7) for $r > r_0$) and the noninteracting wavefunction along either the z - or ρ -directions. For better comparison, we should plot only the s -wave component of the noninteracting wavefunction, but this happens to be very slowly converging numerically. The inclusion of higher-order partial waves thus induces a second-order difference (because $\psi_{2,m}(r) \propto r^2$ for small r), but one can still appreciate the very good matching of the two functions even at these extreme confinements. In contrast, the two functions calculated from the original theory do not match.

The fact that we can gain two orders in the matching procedure by using the free-space expression (7) implies that the replacement $a \rightarrow a(k)$ greatly improves the accuracy and the

range of validity of the original theory. Although we do not have an estimation of the accuracy on g_1 and g_2 , we expect the extended theory to give reasonably good predictions for $\sigma \gtrsim r_0$. This improvement brought by the simple replacement $a \rightarrow a(k)$ is not so surprising in view of the results reported in [13, 15, 21–23], which have shown the relevance of energy-dependent scattering lengths for the accurate calculation of energy levels in 3D confined geometries. It has been long known in other contexts that contact interaction models are significantly improved when the coupling constants are proportional to the energy-dependent scattering length (or reactance matrix) [24]. Similar extensions of (9) and (10) were considered in [25]–[27] in order to take into account the energy dependence due to a scattering resonance at low energy. In [27], a renormalized contact interaction was used, leading to the replacement of a by the quantity $(2\mu/4\pi\hbar^2)T(k)$, where $T(k) = (4\pi\hbar^2/2\mu)a(k)(1 + ika(k))^{-1}$ is the T -matrix. This complex quantity is equivalent to the real $a(k)$ at low energy. Here, we focus on the energy dependence for strong confinement even in the absence of any resonance.

In the quasi-1D ($q_{nm} \ll k$) or quasi-2D ($q_n \ll k$) regimes, the collisional energy is set by the confinement length σ and can be relatively high, although the effective collisions in the weak directions are cold. An interesting consequence of the extended theory is that if the confinement is strong enough, the collisional energy can probe the energy-dependence of $a(k)$. For a standard contact potential [18], $a(k)$ is constant and equal to a . However, a more realistic $a(k)$ has some energy dependence. For instance, in the effective-range approximation, $a(k)$ has the resonant form:

$$a(k) \approx \frac{a}{1 - (1/2)k^2 a r_e}, \quad (11)$$

where r_e is the effective range of the potential [28]. This approximation works well for short-range interactions with a large scattering length $a \gg r_e$. In the case of van der Waals interactions, the effective range r_e is a simple function of a and β_6 [29, 30]

$$r_e = \frac{2}{3} \frac{\beta_6^2}{\bar{a}} \left(\left(\frac{\bar{a}}{a} \right)^2 + \left(\frac{\bar{a}}{a} - 1 \right)^2 \right) \quad (12)$$

where $\bar{a} = 2\pi\beta_6/\Gamma(1/4)^2$. More elaborate analytical expressions of $a(k)$ valid for any a have been derived for van der Waals interactions [30]. The interest of equations (10) and (11) is that they give a simple two-parameter description of the collisions for a wide range of energies.

To illustrate these ideas, we calculated the 1D interaction strength g_{1D} for a van der Waals interaction consistent with the Lennard-Jones parameters of the numerical calculation reported in [14]. The authors observed a difference between their numerical calculation and the analytic formula (9) where a is taken as the zero-energy scattering length. They suggested that this difference comes from the fact that the confinement-induced resonance in g_{1D} results from a Feshbach resonance with a trap bound state, whose binding energy is not predicted accurately by a pseudopotential based only on the scattering length. As a result, the formula (9) does not predict the resonance at the right location. However, we show in figure 2 that the same formula used in conjunction with the replacement $a \rightarrow a(k)$ in the effective range approximation reproduces the numerical calculations very well. This is because the effective range approximation is able to reproduce the binding energy of the last bound state accurately. The only region where the effective range approximation fails is for small scattering lengths $a \ll \beta_6$, where it predicts a spurious resonance, as visible in figure 2.

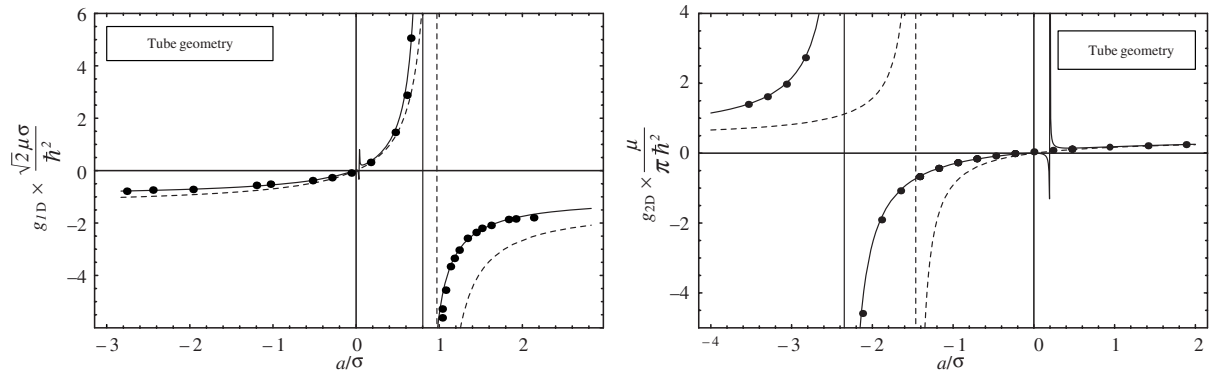


Figure 2. The 1D interaction strength (left panel) and the 2D interaction strength (right panel) in dimensionless units as a function of the ratio of the 3D scattering length a over the confinement dimension σ (a is varied and σ is fixed). As in figure 1, $\sigma = 1.95 \beta_6$ in the left panel and $\sigma = 1.18 \beta_6$ in the right panel. The dots are obtained by numerically solving the problem of two atoms interacting through a Lennard-Jones potential in a 3D cylindrically-symmetric trap; dots in the left panel (tube geometry) were taken from [14] and confirmed by us, while we calculated the dots in right panel (pancake geometry) using the adaptive grid refinement method of [20]. The dashed curves correspond to the formulae (9) and (10) with the zero-energy scattering length a , and the solid curves corresponds to the same formulae using the energy-dependent scattering length $a(k)$ instead of a . Here, $a(k)$ has been calculated in the effective-range approximation, equation (11), which is valid almost everywhere except for small positive scattering lengths where the approximation causes a spurious resonance.

We also calculated the 2D interaction strength and checked that a similar situation occurs in the pancake configuration. Using the adaptive grid refinement method of [20], we solved the Schrödinger equation (1) for a Lennard-Jones interaction $U(r) = (C_{12}/r^{12}) - (C_6/r^6)$ and a cylindrical harmonic trap. The tight pancake limit is obtained by setting the ratio of axial and radial frequencies to 400 (thus leading to a spatial aspect ratio of 1/20), and the tight confinement scale is set to $\sigma = 1.18 \beta_6$. The parameter C_{12} is adjusted to set the number of bound states supported by the interaction and the scattering length. From this calculation, we obtained the eigenenergies and then used equation (21) of [31] to extract the 2D scattering length. We found that it shows very little dependence on the number of bound states, which can be as low as 2, saving computational efforts. Using equation (7) of [19] (or equation (15) of [32]), we could then relate the 2D scattering length to the interaction strength g_{2D} for any q_0 —we chose a q_0 given by the zero-point momentum in the weak direction. Figure (2) compares this numerical g_{2D} with the analytical formula (9) for the same q_0 . Again, the position of the confinement-induced resonance for negative scattering lengths [11] is correctly predicted by (9) provided the energy-dependent scattering length is used. As previously, the effective range approximation works well, except for small scattering lengths. These results also suggest that the observation of the resonance may provide useful information about the effective range of the interaction.

In summary, we have shown that the effective 1D or 2D interactions of ultracold bosons in strongly confined systems are governed by 3D collisions at a relatively high energy determined

by the confinement. The effect of these high-energy collisions can be well described by a single quantity, the energy-dependent scattering length, up to extremely tight confinements. For van der Waals interactions, this quantity itself can be expressed in the effective range approximation in terms of the zero-energy scattering length and the van der Waals length. This parametrized energy-dependent scattering length leads to an accurate analytic prediction of the confinement-induced resonance both in 1D and 2D confinements.

Appendix

In this appendix, we show that for 2D confinement the matching procedure is effective up to second order in the expansion in r/σ near $r = 0$. Without loss of generality, we take the wavefunction to be symmetric around the z -axis (i.e. $m = 0$ in equation (4)), so that equation (6) can be written as

$$\psi(\vec{r}) = \sum_{\ell=0}^{\infty} \psi_{\ell}(r) i^{\ell} (2\ell + 1) P_{\ell}(\cos \theta), \quad (\text{A.1})$$

where $P_{\ell}(x)$ is the Legendre polynomial. The basic approximation is to assume that the components ψ_{ℓ} are proportional to those of the free-space solution. With the assumption that only the s -wave component is scattered by the potential, we set

$$\psi_0(r) = \eta_0 \phi_{n0}(0) [j_0(kr) + ka(k)y_0(kr)] \quad (\text{A.2})$$

$$\psi_{\ell \neq 0}(r) = \eta_{\ell} \phi_{n0}(0) j_{\ell}(kr), \quad (\text{A.3})$$

where j_{ℓ} and y_{ℓ} are the spherical Bessel functions, and η_{ℓ} are factors to be determined. (Note that with this definition, η in equation (7) is equal to $\eta_0 \phi_{n0}(0)$.) Since only components of even ℓ are coupled to the s -wave component by the trapping potential $V(\vec{r})$, we can discard odd- ℓ components (they do not play a role in the scattering process). An expansion near $r = 0$ of equation (A.1) therefore reads

$$\begin{aligned} \phi_{n0}(0) \left[\eta_0 \left(-\frac{ka(k)}{kr} + 1 \right) + \left(\eta_0 \frac{ka(k)}{2} \right) kr - \left(\frac{\eta_0}{6} + \frac{\eta_2}{3} P_2(\cos \theta) \right) (kr)^2 \right. \\ \left. - \left(\eta_0 \frac{ka(k)}{24} \right) (kr)^3 + \dots \right]. \end{aligned} \quad (\text{A.4})$$

This is to be matched with equation (4). Using the explicit form of the harmonic oscillator solutions ϕ_{n0} , it can be written as

$$\phi_{n0}(0) \Upsilon_n \left[\frac{\rho}{\sqrt{2}\sigma}, \frac{z}{\sqrt{2}\sigma}, -\frac{1}{2} q_{00}^2 \sigma^2 \right], \quad (\text{A.5})$$

with

$$\Upsilon_n [u, v, \epsilon] = e^{(-u^2/2)} L_n(u^2) \cosh(2v\sqrt{n+\epsilon}) - \frac{A_{n0}}{\sqrt{2}\sigma} \Lambda [u, v, \epsilon],$$

$$\Lambda [u, v, \epsilon] = \sum_{\nu=0}^{\infty} \frac{e^{-2v\sqrt{v+\epsilon}}}{\sqrt{v+\epsilon}} e^{(-u^2/2)} L_{\nu}(v^2),$$

where the L_ν is the Laguerre polynomial. For equation (A.5) a partial wave expansion appears not feasible, so we resort to evaluating the expressions along the ρ and z -axes. Along the z -axis ($\rho = 0$), we find the following expansion

$$\Lambda[0, v, \epsilon] = \frac{1}{v} + \zeta\left(\frac{1}{2}, \epsilon\right) + (2\epsilon - 1)v + 2\zeta\left(-\frac{1}{2}, \epsilon\right)v^2 + \frac{1}{6}[(2\epsilon - 1)^2 - \frac{1}{3}]v^3 + \dots \quad (\text{A.6})$$

Along the ρ -axis ($z = 0$), we find the following expansion

$$\begin{aligned} \Lambda[u, 0, \epsilon] &= \frac{1}{u} + \zeta\left(\frac{1}{2}, \epsilon\right) + (2\epsilon - 1)u + \left[\frac{1}{2}(2\epsilon - 1)\zeta\left(\frac{1}{2}, \epsilon\right) - \zeta\left(-\frac{1}{2}, \epsilon\right)\right]u^2 \\ &\quad + \frac{1}{6}[(2\epsilon - 1)^2 + \frac{2}{3}]u^3 + \dots \end{aligned} \quad (\text{A.7})$$

In these expansions, ζ refers to the Hurwitz zeta function which we define as follows

$$\zeta(s, \epsilon) = \lim_{N \rightarrow \infty} \sum_{n=0}^N \frac{1}{(n + \epsilon)^s} - \frac{(N + \epsilon + 1/2)^{-s+1}}{-s + 1}$$

for $-1 < s < 1$, generalizing the definition given in [14, 33]. The first expansion (A.6) was found using the counter-term method explained in these references with the refined counter term $\int_0^{N+(1/2)+\epsilon} \frac{\exp(-2\sqrt{sx})}{\sqrt{s}} ds$. The second expansion (A.7) was guessed from the expected result (A.4), and checked numerically. Because of the very slow convergence of the sum in $\Lambda[u, 0, \epsilon]$, we could not check the terms directly. Instead, we noted that the Laplace transform of Λ with respect to the argument u is related to the Lerch transcendent Φ [34]

$$\int_0^\infty e^{-su} \Lambda[u, 0, \epsilon] du = \frac{1}{s + 1/2} \Phi\left(\frac{s - 1/2}{s + 1/2}, \frac{1}{2}, \epsilon\right),$$

and assumed there is a direct correspondence between the Laplace transform of the terms in (A.7) and the terms in the asymptotic expansion of the Laplace transform near $s \rightarrow \infty$.

Matching the expressions (A.4) and (A.5) along the z -direction leads to the following relations for each order of the expansion

$$\eta_0 a(k) = A_{n0}, \quad (\text{A.8})$$

$$\eta_0 = 1 - \frac{A_{n0}}{\sqrt{2}\sigma} \zeta(1/2, \epsilon), \quad (\text{A.9})$$

$$\eta_0 \frac{k^2 a(k)}{2} = \frac{A_{n0}}{2\sigma^2} (k^2 \sigma^2), \quad (\text{A.10})$$

$$\left(\frac{\eta_0}{6} + \frac{\eta_2}{3}\right) k^2 = \frac{k^2}{2} - \frac{1 + 2n}{2\sigma^2} + \frac{A_{n0}}{\sqrt{2}\sigma^3} \zeta(-1/2, \epsilon), \quad (\text{A.11})$$

$$\eta_0 \frac{ka(k)}{24} k^3 = \frac{A_{n0}}{24\sigma^4} (k^4 \sigma^4 - \frac{1}{3}), \quad (\text{A.12})$$

while, matching along the ρ -direction leads to the following relations

$$\eta_0 a(k) = A_{n0}, \quad (\text{A.13})$$

$$\eta_0 = 1 - \frac{A_{n0}}{\sqrt{2}\sigma} \zeta(1/2, \epsilon), \quad (\text{A.14})$$

$$\eta_0 \frac{k^2 a(k)}{2} = -\frac{A_{n0}}{2\sigma^2} (k^2 \sigma^2), \quad (\text{A.15})$$

$$\left(\frac{\eta_0}{6} - \frac{\eta_2}{6} \right) k^2 = \frac{1+2n}{4\sigma^2} - \frac{A_{n0}}{2\sqrt{2}\sigma^3} \left[\frac{k^2 \sigma^2}{2} \zeta(1/2, \epsilon) + \zeta(-(1/2), \epsilon) \right], \quad (\text{A.16})$$

$$\eta_0 \frac{ka(k)}{24} k^3 = \frac{A_{n0}}{24\sigma^4} (k^4 \sigma^4 + 2/3), \quad (\text{A.17})$$

where we make use of $2\epsilon - 1 = -k^2 \sigma^2$. Relations (A.8) and (A.9) and (A.13) and (A.14) are the same and determine A_{n0} and the s -wave factor

$$\eta_0 = \frac{1}{1 + [a(k)/\sqrt{2}\sigma] \zeta[(1/2), -(q_{00}^2 \sigma^2)]} \quad (\text{A.18})$$

Relations (A.10) and (A.15) are the same and are both satisfied with the previous determination of A_{n0} and η_0 . Relations (A.11) and (A.16) are consistent and give the same determination of the d -wave factor

$$\eta_2 = \eta_0 \left(\frac{3a(k)}{\sqrt{2}k^2 \sigma^3} \zeta \left(\frac{1}{2}, -\frac{q_{00}^2 \sigma^2}{2} \right) - \frac{1}{2} \right) + \frac{3}{2} \frac{q_{n0}^2}{k^2}. \quad (\text{A.19})$$

However, neither relation (A.12) or (A.17) are satisfied with the previous determination of A_{n0} and η_0 (because of the terms $-1/3$ and $2/3$), which means that the free-space approximation (A.2) and (A.3) is valid up to order r^2 . The error is $\phi_{n0}(0)|\eta_0 a(k)|\frac{1}{24\sigma^4} r^3$. The range of r for which this error is negligible determines the range $[r_0, r_1]$ where a matching is possible. Since the error increases with r , we can define r_1 as the r for which the ratio between the error and the wavefunction (A.4) is equal to a certain tolerance α . In the limit of large scattering lengths, one finds

$$r_1 = (24\alpha)^{1/4} \sigma.$$

The range $[r_0, r_1]$ where the two functions can be matched to within the tolerance α exists as long as $r_1 > r_0$, i.e.

$$\sigma > (24\alpha)^{-1/4} r_0. \quad (\text{A.20})$$

For instance, for $\alpha = 1\%$, one gets $\sigma > 1.43r_0$. This indicates that the method works even for a confinement length σ on the order of the range r_0 .

We can also check that this is consistent with our assumption that only s -waves are scattered. Higher-order partial wave scattering arises if we take into account the dependence of A_{n0} on ν . The first correction is $A_{n0} \rightarrow A_{n0} + (\nu + 1/2)B_{n0}$, and leads to the term $B_{n0}\sigma^2/z^3$ along the z -axis. This term is to be matched with the leading-order term of the scattered d -wave term $(-K_2)\eta_2\phi_{n0}(0)y_2(kz)(-5)P_2(\cos 0)$, where K_2 is the d -wave reactance matrix element. In the absence of shape resonance, K_2 is purely determined by the long-range van der Waals behaviour of the interaction, $K_2 \approx -\frac{1}{100}(k\beta_6)^4$ —see equation (8) of [30]. This leads to

$$B_{n0} = -\eta_2 \frac{\sigma (k\beta_6)^4}{20 (k\sigma)^3}.$$

d -wave scattering is negligible if $|B_{n0}| \ll |A_{n0}|$. In the quasi-1D regime ($q_{n0} \ll k$ and $k \sim 1/\sigma$), and using the value of η_2 (A.19), one finds

$$\sigma^4 \gg \left(\frac{1}{40}|1 - \sigma/a(k)|\right) \beta_6^4,$$

which for a wide range of scattering lengths is consistent with the condition (A.20) and the cold collision condition $kr_0 < 1$ given in the text.

References

- [1] Görlitz A *et al* 2001 *Phys. Rev. Lett.* **87** 130402
- [2] Denschlag J H, Simsarian J E, Häffner H, McKenzie C, Browaeys A, Cho D, Helmerson K, Rolston S L and Phillips W D 2002 *J. Phys. B: At. Mol. Opt. Phys.* **35** 3095
- [3] Richard S, Gerbier F, Thywissen J H, Hugbart M, Bouyer P and Aspect A. 2003 *Phys. Rev. Lett.* **91** 010405
- [4] Spielman I B, Johnson P R, Huckans J H, Fertig C D, Rolston S L, Phillips W D and Porto J V 2006 *Phys. Rev. A* **73** 020702
- [5] Ido T and Katori H 2003 *Phys. Rev. Lett.* **91** 053001
- [6] Ludlow A D, Boyd M M, Zelevinsky T, Foreman S M, Blatt S, Notcutt M, Ido T and Ye J 2006 *Phys. Rev. Lett.* **96** 033003
- [7] Olshanii M 1998 *Phys. Rev. Lett.* **81** 938
- [8] Petrov D S, Shlyapnikov G and Walraven J T M 2000 *Phys. Rev. Lett.* **85** 3745
- [9] Paredes B, Widera A, Murg V, Mandel O Fälling S, Cirac I, Shlyapnikov G V, Hänsch T W and Bloch I 2004 *Nature* **429** 277
- [10] Kinoshita T, Wenger T and Weiss D S 2004 *Science* **305** 1125
- [11] Petrov D S, Holzmann M and Shlyapnikov G V 2000 *Phys. Rev. Lett.* **84** 2551
- [12] Tiesinga E, Williams C J, Mies F H and Julienne P S 2000 *Phys. Rev. A* **61** 063416
- [13] Blume D and Greene C H 2002 *Phys. Rev. A* **65** 043613
- [14] Bergeman T, Moore M G and Olshanii M 2003 *Phys. Rev. Lett.* **91** 163201
- [15] Bolda E L, Tiesinga E and Julienne P S 2002 *Phys. Rev. A* **66** 013403
- [16] Julienne P S 1996 *J. Res. Natl Inst. Stand. Technol.* **101** 487
- [17] Kim J I, Schmiedmayer J and Schmelcher P 2005 *Phys. Rev. A* **72** 042711
- [18] Fermi E 1934 *Nuovo Cimento.* **11** 157
- [19] Petrov D S and Shlyapnikov G V 2001 *Phys. Rev. A* **64** 012706
- [20] Mitchell W F and Tiesinga E 2005 *Appl. Num. Math.* **52** 235

- [21] Bolda E L, Tiesinga E, and Julienne P S 2003 *Phys. Rev. A* **68** 032702
- [22] Stock R, Silberfarb A, Bolda E L and Deutsch I H 2005 *Phys. Rev. Lett.* **94** 023202
- [23] Idziaszek Z and Calarco T 2006 *Preprint* quant-physics/0604205
- [24] Masnou-Seeuws F 1982 *J. Phys. B: At. Mol. Phys.* **15** 883
- [25] Wouters M, Tempere J and Devreese J T 2003 *Phys. Rev. A* **68** 053603
- [26] Granger B E and Blume D 2004 *Phys. Rev. Lett.* **92** 133202
- [27] Yurovsky V A 2005 *Phys. Rev. A* **71** 012709
- [28] Bethe H A 1949 *Phys. Rev.* **76** 38
- [29] Flambaum V V, Gribakin G F and Harabati C 1999 *Phys. Rev. A* **59** 1998
- [30] Gao B 1998 *Phys. Rev. A* **58** 4222
- [31] Busch T, Englert B-G, Rzčewski K and Wilkens M 1998 *Found. Phys.* **28** 549
- [32] Lee M D, Morgan S A, Davis M J and Burnett K 2002 *Phys. Rev. A* **65** 043617
- [33] Moore M G, Bergeman T and Olshanii M 2004 *J. Phys. IV France* **116** 69 (*Preprint* cond-mat/0210556).
- [34] Erdélyi A, Magnus W, Oberhettinger F and Tricomi F G 1953 *Higher Transcendental Functions* vol 1 (New York: McGraw-Hill)